Chirality-induced spin filtering in pseudo Jahn-Teller molecules

Akihito Kato [1], Hiroshi M. Yamamoto [2], and Jun-ichiro Kishine[1,2]

[1]*Division of Natural and Environmental Sciences, The Open University of Japan, Chiba 261-8586, Japan*
[2]*Research Center of Integrative Molecular Systems, Institute for Molecular Science, Okazaki, Aichi 444-8585, Japan*

Chirality-induced spin selectivity (CISS) refers to an ability to induce a spin polarization of an electron transmitted through chiral materials. An important experimental observation is that incredibly large spin polarization is realized at room temperature even for organic molecules that have weak spin-orbit coupling (SOC), although SOC is the only interaction that can manipulate the electrons' spins in the setups. Therefore the mechanism of the CISS needs to be constructed in a way insensitive to or enhancing the magnitude of the SOC strength. In this paper, we describe a theoretical study of CISS with a model chiral molecule that belongs to the point group C_3. In this molecule, electronic translational and rotational degrees of freedom for an injected electron are coupled to one another via the nuclear vibrational mode with a pseudo Jahn-Teller effect. By properly taking the molecular symmetry as well as the time-reversal symmetry into account and classifying the molecular ground states by their angular- and spin-momentum quantum numbers, we show that the chiral molecule can act as an efficient spin filter. The efficiency of this spin filtering can be nearly independent of the SOC strength in this model, while it well exceeds the spin polarization relying solely on the SOC. The nuclear vibrations turned out to have the role of not only mediating the translation-rotation coupling, but also enhancing the spin-filtering efficiency.

I. INTRODUCTION

An object that cannot be overlapped with its mirror images, namely, that lacks the reflection symmetries, is called chiral. The chiral symmetry breaking gives rise to abundant functionality [1] such as chiral magnetism [2,3], chiral phononics [4–6], chiral photonics [7], and nonreciprocal conductivity [8,9]. Recent experimental observations have confirmed that the chiral materials exhibit spin-selective phenomena, including a large spin polarization of photoelectrons transmitted through helical molecules [10–12] and a large spin dependence of the current-voltage characteristics for the tunneling electrons through helical molecules [13–15]. Even enantioseparation and asymmetric electrochemical reactions by magnetic electrodes are reported [16,17]. Furthermore, generation of large spin current was established for the inorganic chiral crystals [18–20]. These phenomena that originate from the structural chirality are collectively termed the chirality-induced spin selectivity (CISS) [21–24], where the spin is oriented parallel or antiparallel to the velocity of an injected electron depending on the materials' handedness.

CISS has been actively studied and become an interdisciplinary research field spanning physics, chemistry, and biology. The reported spin polarization up to 60% amounts to an effective magnetic field of the order of 100 T [21], which is unrealistically strong. So far, theoretical attempts have been made based on the electron motion in a chiral molecule in the presence of spin-orbit coupling (SOC) with dephasing [25,26] or nonunitary [27] effect. These attempts have been made partly because of the necessity of removing the restriction made by the Bardarson theorem [28], in which no spin

polarization is allowed due to time-reversal symmetry when two-terminal scattering centers without leakage are considered, which is, however, not always the case as demonstrated for a two-channel model [29]. Recently, the importance of couplings of electronic or other degrees of freedom has been proposed, including the Coulomb interactions [30], the nuclear vibrations and polarons [31–33], and substrate-molecule interface effects [34]. In order to find an alternative explanation, we would like to understand the fact that the CISS effect is observed even in organic molecules with weak SOC strength in a way that does not rely explicitly on the strength of the SOC. To do so, we hypothesize that interplay between nuclear and electronic motions which are governed by the same symmetry restrictions in chiral materials has a critical role in the CISS effect, where the leakage is replaced with a built-in molecular degree of freedom rather than an external outlet.

For our purpose, we consider a molecule under the pseudo Jahn-Teller effect [35,36], where the coupling between an electronic translation and rotation is mediated by the nuclear vibrational degrees of freedom. The Hamiltonian that includes the electron-nuclear coupling and the SOC satisfies the time-reversal symmetry. This symmetry confirms that the up-spin and the down-spin states are degenerate forming a Kramers pair. The members of this degenerate pair can be separated from each other by its translational direction, which is made possible by the pseudo Jahn-Teller coupling. Consequently, the chiral molecule acts as the spin filter by introducing the spin-selective electron injection from an external source, which is distinct from the spin-polarizing effect during propagation in the molecule. The coexistence of the SOC and the

(pseudo) Jahn-Teller coupling has an intricate effect on the existence of the orbital degeneracy or the conical intersection [37,38]. However, this is essentially irrelevant to the spin-filtering effect proposed in this paper. We further demonstrate that the performance of this chiral spin filter is determined critically by the spin-selective transmission probability. In this model, angular-momentum (AM) quantum numbers play a crucial role in obtaining quite large efficiency insensitive to the SOC strength.

The remaining part of this paper is organized as follows: In Sec. II, we introduce the model Hamiltonian of a chiral molecule which belongs to the point group C_3. In Sec. III, we propose the spin-filtering mechanism of the chiral molecule based on the classification of eigenstates by the AM and discuss its condition in Sec. IV. In Sec. V, we mention the nuclear vibrational role in the efficient spin filtering. Section VI is devoted to the concluding remarks.

II. MODEL

A. Molecular basis

Molecular symmetry shapes a potential field that is exerted on an electron injected into the molecule to create a rotational motion from the translational one. As a result, the molecular orbital occupied by the injected electron is spanned by both the translational and rotational basis. This study focuses on the point group C_3 as the minimal point group that allows chiral structure and has a rotational basis with the one rotating in a direction opposite to the other. Extending the model to the other point groups C_n with $n \geqslant 4$ is straightforward. Let the z axis be the threefold rotation axis. We write $|\phi_z\rangle$ for the translational state that is transformed as z, and $|\bar{\phi}_z\rangle := \Theta|\phi_z\rangle$ for its time reversal with Θ being the time-reversal operator. Inclusion of $|\bar{\phi}_z\rangle$ allows us to construct the model Hamiltonian that satisfies the time-reversal symmetry in an unambiguous way. Obviously, $\langle\phi_z|\hat{p}_z|\phi_z\rangle = -\langle\bar{\phi}_z|\hat{p}_z|\bar{\phi}_z\rangle$ holds, where $\hat{p}_z$ is the z component of the electron momentum operator, and $\langle\phi_z|\hat{p}_z|\phi_z\rangle > 0$ is assumed. Because these bases belong to the A irreducible representation of the point group C_3, they are invariant under the threefold rotation C_3. The bases for the rotation on the xy plane, which belong to the E_1 and E_2 irreducible representations, are denoted by $|\phi_\pm\rangle$. These rotational states are transformed under C_3 and Θ as

$$C_3|\phi_\pm\rangle = e^{\mp i2\pi/3}|\phi_\pm\rangle \tag{1}$$

and

$$\Theta|\phi_\pm\rangle = |\phi_\mp\rangle, \tag{2}$$

respectively.

In chiral materials, translational and rotational motions are coupled with each other [1]. However, in our model, the coupling between the translational and rotational states of an electron is mediated by the nuclear vibrational modes belonging to the e_1 and e_2 representation. Indeed, the product representation $e_i \times E_i$ for $i = 1, 2$ includes the A representation. Consequently, there arises a finite matrix element $\langle A|e_i|E_i\rangle$ in a symbolic form. The nuclei in the $e_{1,2}$ representation also induce the coupling between the rotational states. This coupling between degenerate rotational states causes the spontaneous distortion, which is known as the Jahn-Teller

effect [35,36]. The coupling between nondegenerate (E_i and A) states can also cause a similar symmetry breaking called the pseudo Jahn-Teller effect [35,36]. The nuclear coordinates in the $e_{1,2}$ representation are written as $Q_\pm = \rho e^{\pm i\varphi}$ with the radius ρ and the angle φ. The symmetry operations transform $Q_\pm$ in the following way:

$$C_3 Q_\pm = e^{\pm i2\pi/3} Q_\pm \tag{3}$$

and

$$\Theta Q_\pm = Q_\mp. \tag{4}$$

To describe the spin-dependent process, the electronic spin must be added to the basis. Let $|\uparrow\rangle$ and $|\downarrow\rangle$ denote the up-spin and down-spin states, respectively. They are transformed under the symmetry operations as

$$C_3|\uparrow/\downarrow\rangle = e^{\mp i\pi/3}|\uparrow/\downarrow\rangle \tag{5}$$

and

$$\Theta|\uparrow/\downarrow\rangle = \pm|\downarrow/\uparrow\rangle. \tag{6}$$

B. Model Hamiltonian

The Hamiltonian, H, describing an electron propagating through the chiral molecule consists of the electronic H_e, the nuclear H_n, and the electron-nuclear coupling H_{en} Hamiltonians, which are all spin independent, and the SOC Hamiltonian H_{soc}, $H = H_e + H_n + H_{en} + H_{soc}$. The electronic Hamiltonian is given by

$$H_e = \epsilon_{tr}(|\phi_z\rangle\langle\phi_z| + |\bar{\phi}_z\rangle\langle\bar{\phi}_z|) + \epsilon_{rot}(|\phi_+\rangle\langle\phi_+| + |\phi_-\rangle\langle\phi_-|), \tag{7}$$

where we set $\epsilon_{rot} \equiv 0$ throughout the paper, and the nuclear Hamiltonian is described as the two-dimensional harmonic oscillator,

$$H_n = -\frac{\hbar^2}{2M}\left(\frac{1}{\rho}\frac{\partial}{\partial\rho}\rho\frac{\partial}{\partial\rho} + \frac{1}{\rho^2}\frac{\partial^2}{\partial\varphi^2}\right) + \frac{M\omega^2}{2}\rho^2, \tag{8}$$

where M and ω are the nuclear mass and frequency and $\hbar$ is Planck's constant. For derivation of H_{en}, we use the symmetry conditions $[H_{en}, C_3] = [H_{en}, \Theta] = 0$ and take only the first order in $Q_\pm$, which becomes (see Ref. [39] and Appendix A for details)

$$\begin{aligned}
H_{en} = {} & V_+ Q_- |\phi_z\rangle\langle\phi_+| + V_- Q_+ |\phi_z\rangle\langle\phi_-| \\
& + V_-^* Q_- |\bar{\phi}_z\rangle\langle\phi_+| + V_+^* Q_+ |\bar{\phi}_z\rangle\langle\phi_-| \\
& + V_0 Q_- |\phi_+\rangle\langle\phi_-| + \text{H.c.}, \tag{9}
\end{aligned}$$

where H.c. stands for the Hermitian conjugate of all the preceding terms. The first and second lines of the right-hand side of Eq. (9) represent the translation-rotation coupling with its strength $V_\pm$, and the third line represents the rotation-rotation coupling with the coupling strength V_0. Without loss of generality, these coupling constants can be always set to be real.

Here, we stress that the chirality imposes

$$V_+ \neq V_-. \tag{10}$$

Actually, the reflection symmetry leads to $V_+ \equiv V_-$. We see this by adding a vertical mirror, i.e., considering the case of the point group C_{3v}. In this case, the reflection operator σ_v

acts on the molecular basis as $\sigma_v|\phi_\pm\rangle = |\phi_\mp\rangle$, $\sigma_v Q_\pm = Q_\mp$, and $\sigma_v|\uparrow/\downarrow\rangle = \pm|\downarrow/\uparrow\rangle$.

The only ingredient for the spin-dependent process in our model is the SOC. The derivation of H_{soc} is similar to that of H_{en} (see Ref. [38] and Appendix B for details): We use the symmetry conditions $[H_{soc}, K] = 0$ for $K = C_3$ and Θ. For simplicity, we retain only the zeroth-order terms in $Q_\pm$,

$$H_{soc} = \lambda(|\phi_+\rangle\langle\phi_+| - |\phi_-\rangle\langle\phi_-|) \otimes \hat{\sigma}_z, \qquad (11)$$

with $\hat{\sigma}_z = |\uparrow\rangle\langle\uparrow| - |\downarrow\rangle\langle\downarrow|$ and the SOC strength λ. Equation (11) indicates that spin-momentum locking works in the chiral molecule: In the cases of $V_+ > V_-$ and $V_+ < V_-$, the electron propagated with the positive momentum stabilizes the counterclockwise ($|\phi_+\rangle$) and clockwise ($|\phi_-\rangle$) rotations, respectively. For $\lambda > 0$, this counterclockwise (clockwise) rotation stabilizes the down-spin (up-spin) state. Here, we note that we neglect the spin-flipping components of H_{soc} by disregarding the nuclear dependent contributions. This treatment is consistent with the experimental observation [40] that the spin does not flip in the molecule, which may be attributed to the large spin energy difference [18]. It should be pointed out, however, that such spin-flipping components may be relevant to some of the CISS experiments [18–20]. This point will be discussed in a later part of this paper.

C. Observables

To numerically solve the Schrödinger equation for H, we need the nuclear eigenstates $\{|n, m\rangle\}$ to evaluate the matrix elements of H [41,42]. Then, the product state composed of the chiral molecule and injected electron is written as $|\Psi\rangle = \sum_{a=z,\bar{z},+,-} \sum_{s=\uparrow,\downarrow} \sum_{n,m} C_{n,m}^{(a,s)}|\phi_a, s\rangle|n, m\rangle$ with $C_{n,m}^{(a,s)}$ being the coupling coefficient ($\phi_{\bar{z}} \equiv \bar{\phi}_z$ is used for convenience). The electron linear momentum and nuclear AM of $|\Psi\rangle$, which is analyzed later, are calculated from $P = \langle\Psi|\hat{p}_z|\Psi\rangle = g\langle\phi_z|\hat{p}_z|\phi_z\rangle$, where the momentum factor $g = \sum_{s,n,m}[|C_{n,m}^{(z,s)}|^2 - |C_{n,m}^{(\bar{z},s)}|^2]$, and $L_n = \langle\Psi|(-i\hbar\partial_\varphi)|\Psi\rangle = \sum_{a,s,n,m} m\hbar|C_{n,m}^{(a,s)}|^2$, respectively, as derived in Appendix C. Hereinafter, the parameter values for the energy and coupling constants are given in units of $\hbar\omega$ and $(M\omega/\hbar)^{1/2}$, respectively.

III. SPIN-SELECTIVE FILTERING EFFECT

A. Chirality-induced spin filtering

The absence of the spin-flipping components in H_{soc} indicates that the injected electron passes through the molecule without changing its spin. This enables us to propose that the chiral molecule can act as the spin filter: Suppose that one of the ground states, $|\Psi\rangle$, has positive momentum, $P = \langle\Psi|\hat{p}_z|\Psi\rangle > 0$, and a down spin. Due to the time-reversal invariance of H, $\Theta|\Psi\rangle$ is degenerate with $|\Psi\rangle$ but has negative momentum and an up spin. Thus these states form a Kramers pair. In injecting a down-spin electron with $P > 0$ into the molecule, the electron propagates in accordance with $|\Psi\rangle$, the lowest state among eigenstates with the down spin, to succeed in passing through the molecule because of the positivity of the momentum. In contrast, the injected up-spin electron with positive P propagates in accordance with $\Theta|\Psi\rangle$ and not with $|\Psi\rangle$ due to the mismatch of the spin. However, because the
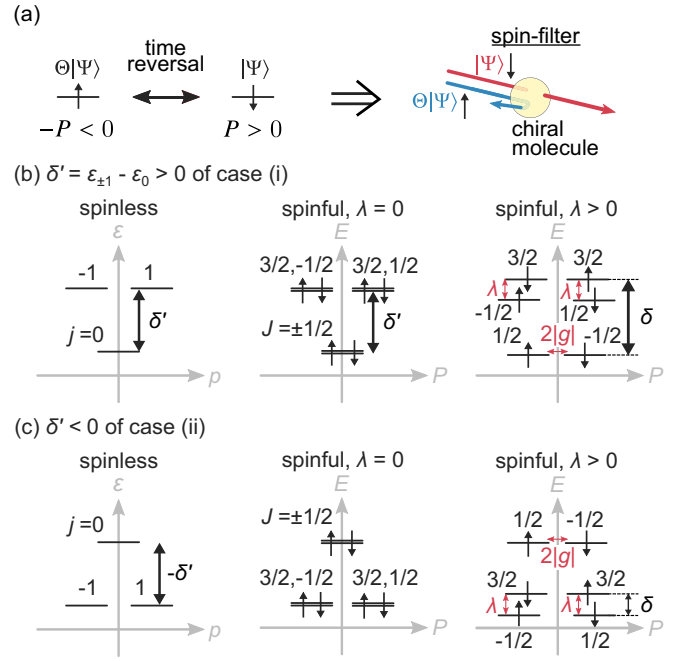

FIG. 1. (a) Schematic picture of the spin filter of chiral molecules. (b) and (c) Energy-momentum diagrams of spinless, spinful with $\lambda = 0$, and spinful with $\lambda > 0$ systems for (b) $\delta' = \epsilon_{\pm 1} - \epsilon_0 > 0$ of case (i) and (c) $\delta' < 0$ of case (ii). Up arrows and down arrows represent the up spin and down spin, respectively.

momentum of $\Theta|\Psi\rangle$ is negative, the up-spin electron cannot pass through the molecule [see Fig. 1(a) for a schematic picture]. Therefore the spin is selectively filtered depending on the translational direction of the lowest eigenstate with the same spin as the injected one. It is of particular importance that this mechanism of selective spin filtering requires the molecule to be chiral. An achiral molecule with $V_+ = V_-$ has a Hamiltonian that is invariant under the exchange of $|\phi_z\rangle$ and $|\bar{\phi}_z\rangle$, physically corresponding to the z-inversion invariance of the system. This invariance causes the disappearance of the momentum, $\langle\Psi|\hat{p}_z|\Psi\rangle \equiv 0$, which means that achiral molecules cannot utilize the translational direction of each eigenstate to filter the electronic spins. Therefore the spin filtering is the chirality-induced effect. Note that this filtering effect efficiently works only when the lowest state for the down spin propagating in the positive translational direction is energetically well separated from that for the up spin. We call their energy difference the spin barrier difference (SBD), denoted by δ, and explore the condition that the SBD becomes large enough to explain CISS not relying on the SOC strength λ.

In what follows, we consider the chiral case only, and without loss of generality, $V_+ > V_- > 0$ is assumed.

B. Classification of eigenstates by AM quantum number

The fact that C_3 commutes with H allows us to classify all the energy eigenstates by their AM quantum number J. We write $|\Psi_J\rangle$ for the energy eigenstate with the AM quantum number J, which satisfies the eigenvalue equations $H|\Psi_J\rangle = E_J|\Psi_J\rangle$ and $C_3|\Psi_J\rangle = e^{-i2\pi J/3}|\Psi_J\rangle$ with $J = 0, \pm 1$ for the
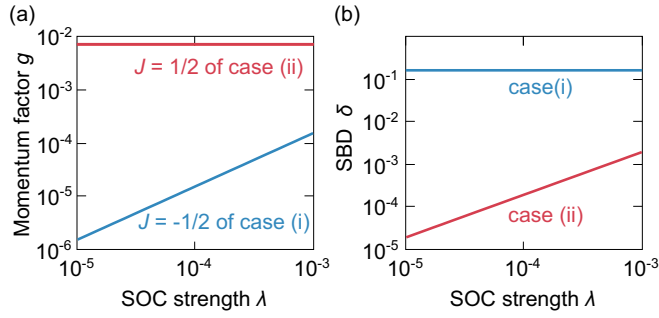
FIG. 2. (a) The momentum factor g of the ground state for cases (i) and (ii) is plotted as a function of the SOC strength λ. Momentum scales linearly for case (i), whereas it is nearly independent of λ for case (ii). (b) The SBDs $\delta \equiv E_{3/2} - E_{-1/2}$ for case (i) and $\delta \equiv E_{3/2} - E_{1/2}$ for case (ii) are plotted as a function of λ.

FIG. 3. (a) The energy differences of the spinless system $\epsilon_1 - \epsilon_0$ are plotted as a function of V_0 for $V_+ = 1$ and $V_+ = 1.5$ with fixed $V_- = 0.5$ and $\Delta = 0.1$. (b) The energy differences of the spinless system $\epsilon_1 - \epsilon_0$ are plotted as a function of ϵ_{tr} for various values of $V_\pm$ with fixed $V_0 = 0.5$.

spinless systems and $J = \pm 1/2, 3/2$ for the spinful systems. Note that J is determined up to the integer multiple of 3, and thus $J = -3/2$ is equivalent to $J = 3/2$. From the time-reversal invariance, $|\Psi_J\rangle$ and $|\Psi_{-J}\rangle$ are degenerate, but with the opposite momentum and spin from each other, immediately leading to $\langle \Psi_0 | \hat{p}_z | \Psi_0 \rangle = 0$.

Now, we consider the effect of small but finite λ on the eigenstates. For distinction, we use a capital J and small letters j for the quantum number in the spinful and spinless systems, respectively, and corresponding state, energy, and momentum are denoted by $|\Psi_J\rangle$, E_J, and P_J for the spinful systems and $|\psi_j\rangle$, ϵ_j, and p_j for the spinless systems, respectively. Two quantum numbers are related by $J = j + 1/2$ for an up spin and $J = j - 1/2$ for a down spin. In the cases of $\lambda = 0$, the spinful states are given by $|\Psi_{j+1/2}\rangle \equiv |\psi_j\rangle|\uparrow\rangle$ or $|\Psi_{j-1/2}\rangle \equiv |\psi_j\rangle|\downarrow\rangle$, where the spatial part of the states is exactly the spinless state $|\psi_j\rangle$, indicating that $E_{j\pm1/2} \equiv \epsilon_j$ and $P_{j\pm1/2} \equiv p_j$. In contrast, in the cases of $\lambda > 0$, where the spatial part of $|\Psi_{j+1/2}\rangle$ is modified from $|\psi_j\rangle$, these states have different energy and momentum; for $j = 0$, the states with $J = \pm1/2$ are degenerate (interchanged by the time-reversal operation) and $P_{\pm1/2} \neq 0$ due to finite λ, as seen in Fig. 2(a), where the momentum factor g scales linearly with λ. The spin direction of the state is governed by the spin-momentum locking. For $\lambda > 0$ and $V_+ > V_-$, the momentum of the down spin, namely, the state with $J = -1/2$, is positive. For $j = 1$ with $p_1 = -p_{-1} > 0$ in the case of $V_+ > V_-$, the spin-momentum locking stabilizes the down-spin state, namely, $E_{3/2} > E_{1/2}$. The origin of the energy splitting in these states is the SOC.

C. SBD

Based on the above argument, we examine the SBD in the cases of (i) $\delta' := \epsilon_1 - \epsilon_0 > 0$ and (ii) $\delta' < 0$. In case (i) [see Fig. 1(b) for a schematic picture], the chiral molecule filters the spin with the ground states $|\Psi_{0\pm1/2}\rangle$. The SBD is, then, given by $\delta \equiv E_{3/2} - E_{-1/2} = \delta' + O(\lambda)$. Hence, under the condition that δ' is much larger than the contribution from the SOC, the SBD is approximated as $\delta \approx \delta'$ and can be nearly independent of λ, as numerically shown in Fig. 2(b). This condition will be discussed later. We propose that the efficient spin-filtering effect exactly corresponds to this situation,
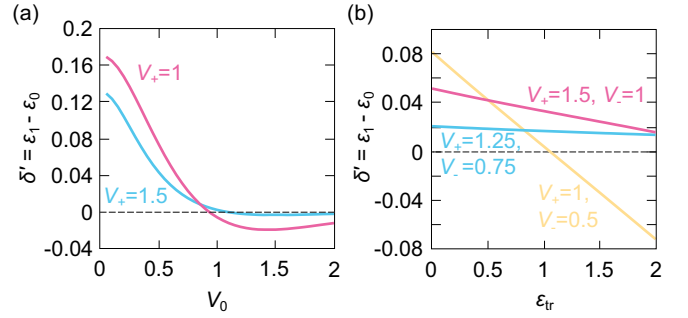
where the effect is insensitive to the magnitude of λ. On the other hand, in case (ii) [see Fig. 1(c) for a schematic picture], the spin filtering occurs in the ground states $|\Psi_{1/2=1-1/2}\rangle$ and $|\Psi_{-1/2=-1+1/2}\rangle$. The SBD is then identical to $\delta \equiv E_{3/2} - E_{1/2} = O(\lambda)$, which is the energy difference caused by the SOC and thus scales linearly with λ as presented in Fig. 2(b). Therefore the resultant spin-filter efficiency is expected to be small.

IV. GROUND STATE OF SPINLESS SYSTEMS

We justify the conditions under which case (i) [Fig. 1(b)] holds, namely, $|\psi_0\rangle$ becomes the ground state for the spinless systems. We start this by presenting two limits in which we can analytically identify the AM quantum number of the ground state. The first is the limit of $V_0 \equiv 0$, where the coupling between the rotational states disappears and only the translation-rotation coupling exists. In this limit, $\hat{l}_1 = -i\hbar\partial_\varphi - \hbar(|\phi_+\rangle\langle\phi_+| - |\phi_-\rangle\langle\phi_-|)$ is conserved with the integer eigenvalue $l_1/\hbar \in \mathbb{Z}$. Among them, the ground state is the state with $l_1 = 0$ that is simultaneously the eigenstate of C_3 with $j = 0$ (the proof of this statement is given in Appendix D). Hence the ground state is given by $|\psi_0\rangle$ in this limit. The second limit is the limit of $V_\pm \to 0$, where the translation and rotation are decoupled, which means that the injected electron directly passes through or is simply circulating in the molecule. In this limit, $\hat{l}_2 = -i\hbar\partial_\varphi + (\hbar/2)(|\phi_+\rangle\langle\phi_+| - |\phi_-\rangle\langle\phi_-|)$ is conserved with the half-odd-integer eigenvalue $l_2/\hbar = \pm(2n-1)/2$ with $n \in \mathbb{N}$. The ground states are given by the states with $l_2/\hbar = \pm1/2$ that are simultaneously the eigenstates of C_3 with $j = \pm1$. Therefore, in this limit, $|\psi_{\pm1}\rangle$ is the ground state.

General situations are located in between these two limits, and the ground states are interchanged depending on the parameter values of ϵ_{tr}, $V_\pm$, and V_0. Figure 3(a) presents the energy difference δ' as a function of the rotational coupling constant V_0. As V_0 is decreased below 0.5, in which the situation approaches the first limit, δ' increases, thus strongly stabilizing the ground state with $j = 0$. Decreasing ϵ_{tr} and/or increasing $V_\pm$ also make the system approach the first limit, in which the translation and rotation are strongly coupled.
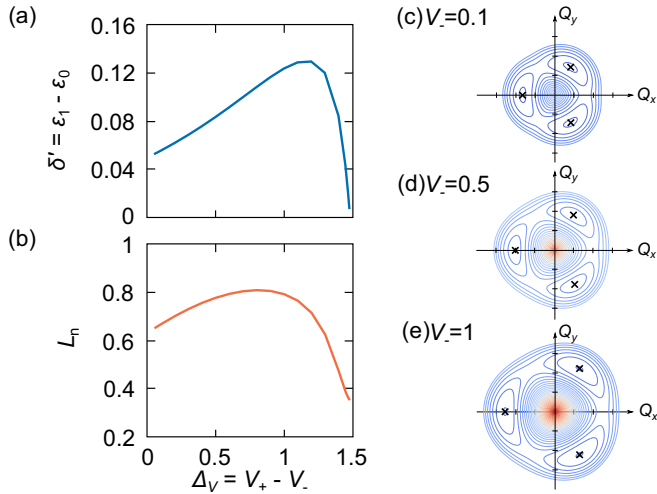
FIG. 4. (a) Energy difference $\delta' = \epsilon_1 - \epsilon_0$ and (b) nuclear AM L_n of $|\psi_1\rangle$ are plotted as a function of $\Delta_V = V_+ - V_-$ with fixed V_+. Other parameters are set to $\epsilon_{tr} = 0.1$ and $V_+ = 1.5$. (c)–(e) Ground-state Born-Oppenheimer potential surfaces are depicted for $V_- = 0.1$ (c), 0.5 (d), and 1 (e). Crosses mark the location of the minimal points in each potential surface, which are farther from the origin as V_- increases.

Therefore the ground state is again given by $|\psi_0\rangle$, which is consistent with the numerical result presented in Fig. 3(b).

V. ROLE OF NUCLEAR AM

Finally, we mention that the energy difference δ' is correlated with that of the nuclear AM. Figures 4(a) and 4(b) present the energy difference $\delta' = \epsilon_1 - \epsilon_0$ and the nuclear AM, $L_n = \langle\psi_1|(-i\hbar\partial_\varphi)|\psi_1\rangle$, respectively, as a function of $\Delta_V := V_+ - V_-$ with fixed V_+. The behavior in Figs. 4(a) and 4(b) can be accounted for by an interplay between the nuclear rotational energy and the pseudo Jahn-Teller effect. In the $\Delta_V < 0.5$ region in Fig. 4(a), as Δ_V increases, this imbalance increases the nuclear AM and further differentiates $|\psi_{\pm1}\rangle$ from $|\psi_0\rangle$, thus increasing δ'. However, increasing Δ_V by decreasing V_- also diminishes the pseudo Jahn-Teller effect, making the nuclear stable configuration close to the high-symmetry point, $\rho \equiv 0$, and hence reducing the nuclear average radius [see Figs. 4(c)–(e)], which leads to the decrease in the nuclear AM and, thus, the nuclear rotational energy. The resultant energy difference decreases as presented in the large-Δ_V region ($\Delta_V > 1.2$) in Fig. 4(a). Therefore the nuclear vibrations have the role of not only mediating the translation-rotation coupling, but also increasing the energy difference δ', and consequently enhancing the spin-filtering efficiency.

VI. CONCLUDING REMARKS

In this paper, we have theoretically explored the mechanism of the spin-filtering effect of chiral molecules. For that purpose, we have constructed a model of the point group C_3 that consists of the electronic translational and rotational states, which are coupled with each other by the pseudo Jahn-Teller effect, or being mediated by the nuclear

vibrational degrees of freedom. The time-reversal symmetry of the Hamiltonian makes it possible to possess, in combination with SOC, spin-momentum locking to filter the injected spin depending on the translational direction. Only when the injected spin state matches the lowest eigenstate of the same translational direction can the electron selectively pass through the molecule with the ground-state energy. This also enables us to classify the molecular eigenstates by their AM quantum number. When the spinless system has a ground state with $j = 0$, the SBD that determines the spin-filter efficiency is nearly independent of the SOC strength, and this makes it possible for the chiral molecule to act as an efficient spin filter protected by the energy for AM quantization. Here we stress that δ' can be estimated at around 50 meV, which is about twice as large as room-temperature energy and is therefore enough to explain the 60% spin polarization in the photoelectron spectroscopy. In the above estimate, as an example, we employed $\hbar\omega = 0.34$ eV (~ 2740 cm^{-1}) in Ref. [43] and a maximum reduced δ' value of 0.16 in Fig. 3(a). The ground state with $j = 0$ for the spinless systems is obtained when the translation-rotation coupling constant $V_\pm$ is sufficiently large compared with the rotational one, V_0. In our future work, the relation between the model parameters and the molecular structure should be clarified together with the direct estimation of the spin-filtering efficiency for actual chiral molecules. Additionally, the mechanism of the spin-filtering proposed in this paper is not the specific property of the point group C_3 and needs to be straightforwardly generalized to other point or space groups to which many chiral and/or gyrotropic materials belong.

In this paper, we have omitted the spin-flipping components from the SOC, which may have a role in diminishing the spin-filtering effect to some extent, because SBD in the present example is large enough to justify such a treatment. From an experimental point of view, this situation is fitting, for example, for the photoelectron transmission through DNA molecules, where the electron is injected from an external source. However, a chirality-induced bulk magnetization of $CrNb_3S_6$ seems to require mechanisms that include the spin-polarizing effect [19]. Therefore CISS seems to include both spin-filtering and spin-polarizing effects depending on the situation. In our model, as given explicitly in Appendix B, we are also able to allow the nuclear-dependent SOC come into play, yielding spin-flipping terms such as $(|\phi_+\rangle\langle\phi_+| - |\phi_-\rangle\langle\phi_-|) \otimes Q_+\hat{\sigma}_+$ and $(|\phi_z\rangle\langle\phi_z| - |\bar{\phi}_z\rangle\langle\bar{\phi}_z|) \otimes Q_+\hat{\sigma}_+$ with $\hat{\sigma}_+ = |\uparrow\rangle\langle\downarrow|$ and $\hat{\sigma}_- = |\downarrow\rangle\langle\uparrow|$. These terms allow AM transfer from nuclear phonon to electron spin, thus polarizing the spin in the chiral molecule while respecting the conservation of AM. This AM conversion may be further enhanced when the molecule involves conical intersections on the adiabatic potential energy surfaces [44,45]. We here note that the current-induced magnetization phenomenon, called the Edelstein effect, is apparently similar to the CISS effect from a global symmetry viewpoint. This effect is, however, interpreted as being mainly dominated by orbital effects [46,47], and the resultant magnetization is much weaker than the huge polarization caused by the CISS effect. The relevance of the spin-flipping components of the SOC to the spin-polarizing effect will be focused on in future studies.

APPENDIX A: DERIVATION OF ELECTRON-NUCLEAR COUPLING HAMILTONIAN

In this Appendix, we derive the electron-nuclear coupling Hamiltonian H_{en} following Ref. [39]. The electron-nuclear coupling Hamiltonian H_{en} is expanded in terms of the electronic basis $\{\phi_z, \phi_{\bar{z}} = \bar{\phi}_z, \phi_+, \phi_-\}$,

$$H_{en} = \sum_{a \neq b = z, \bar{z}, +, -} H_{ab}(Q_+, Q_-)|\phi_a\rangle\langle\phi_b|, \quad (A1)$$

where $H_{ab} = \langle\phi_a|H_{en}|\phi_b\rangle = H_{ba}^*$ is the nuclear-dependent matrix element. First, we impose time-reversal symmetry on H_{en}. The time-reversal operation Θ transforms H_{en} as

$$\Theta H_{en}\Theta^{-1} = \sum_{a,b}(\Theta H_{ab})|\Theta\phi_a\rangle\langle\Theta\phi_b| = \sum_{a,b}H_{ab}^*|\Theta\phi_a\rangle\langle\Theta\phi_b|. \quad (A2)$$

Hence the invariance condition $\Theta H_{en}\Theta^{-1} \equiv H_{en}$ ensures that the matrix elements must satisfy

$$H_{\bar{z}-} = H_{z+}^*, \quad H_{\bar{z}+} = H_{z-}^*. \quad (A3)$$

In the same manner, the invariance condition under the three-fold rotation, $C_3 H_{en}C_3^{-1} \equiv H_{en}$, is equivalent to

$$C_3 H_{z+} = e^{-i2\pi/3}H_{z+}, \quad C_3 H_{z-} = e^{i2\pi/3}H_{z-}, \quad (A4)$$

$$C_3 H_{+-} = e^{-i2\pi/3}H_{+-}. \quad (A5)$$

The explicit form of the matrix elements that satisfy Eq. (A5) is given within the first order of $Q_\pm$ as $H_{z+} = V_+ Q_-$, $H_{z-} = V_- Q_+$, and $H_{+-} = V_0 Q_-$. Consequently, the electron-nuclear coupling Hamiltonian is obtained as

$$\begin{aligned} H_{en} = & V_+ Q_-|\phi_z\rangle\langle\phi_+| + V_- Q_+|\phi_z\rangle\langle\phi_-| \\ & + V_-^* Q_-|\bar{\phi}_z\rangle\langle\phi_+| + V_+^* Q_+|\bar{\phi}_z\rangle\langle\phi_-| \\ & + V_0 Q_-|\phi_+\rangle\langle\phi_-| + \text{H.c.}, \end{aligned} \quad (A6)$$

where H.c. stands for the Hermitian conjugate of all the preceding terms.

APPENDIX B: DERIVATION OF SPIN-ORBIT COUPLING HAMILTONIAN

This Appendix serves as the derivation of the spin-orbit coupling (SOC) Hamiltonian following Ref. [38]. We employ the Breit-Pauli SOC Hamiltonian, which can be effectively reduced to a one-electron Hamiltonian and is expanded in terms of the electronic and spin bases as

$$H_{soc} = \sum_{a,b=z,\bar{z},+,-} \sum_{s_a,s_b=\uparrow,\downarrow} f_{as_a,bs_b}|\phi_a, s_a\rangle\langle\phi_b, s_b|. \quad (B1)$$

For simplicity, we neglect the matrix elements between the electronic translational and rotational states, because the transitions between the nondegenerate states are less probable than those between the degenerate states. For systems with an odd number of electrons, the time-reversal operator satisfies $\Theta^2 = -1$, from which the relation for the matrix element of the spin-orbit coupling Hamiltonian

$$\langle\phi_a, s_a|H_{soc}\Theta|\phi_b, s_b\rangle = -\langle\phi_b, s_b|H_{soc}\Theta|\phi_a, s_a\rangle \quad (B2)$$

is derived. This is equivalent to

$$\begin{aligned} f_{z\uparrow,\bar{z}\downarrow} &= f_{z\downarrow,\bar{z}\uparrow} = f_{\bar{z}\uparrow,z\downarrow} = f_{\bar{z}\downarrow,z\uparrow} \\ &= f_{+\uparrow,-\downarrow} = f_{+\downarrow,-\uparrow} = f_{-\uparrow,+\downarrow} = f_{-\downarrow,+\uparrow} = 0 \end{aligned} \quad (B3)$$

and

$$\begin{aligned} f_{z\uparrow,\bar{z}\uparrow} &= f_{z\downarrow,\bar{z}\downarrow}, \quad f_{z\uparrow,z\downarrow} = -f_{\bar{z}\uparrow,\bar{z}\downarrow}, \\ f_{z\uparrow,z\uparrow} &= f_{z\downarrow,\bar{z}\downarrow}, \quad f_{z\downarrow,z\downarrow} = f_{\bar{z}\uparrow,\bar{z}\uparrow}, \\ f_{z\downarrow,z\uparrow} &= -f_{\bar{z}\downarrow,\bar{z}\uparrow}, \quad f_{\bar{z}\uparrow,z\uparrow} = f_{z\downarrow,\bar{z}\downarrow}, \\ f_{+\uparrow,-\uparrow} &= f_{+\downarrow,-\downarrow}, \quad f_{+\uparrow,+\uparrow} = -f_{-\uparrow,-\downarrow}, \\ f_{+\downarrow,+\downarrow} &= -f_{-\uparrow,-\downarrow}, \quad f_{+\downarrow,+\uparrow} = -f_{-\downarrow,-\uparrow}, \\ f_{-\uparrow,+\uparrow} &= f_{-\downarrow,+\downarrow}. \end{aligned}$$

Next, the Wigner-Eckart theorem can rewrite the matrix element as

$$\langle\phi_a\uparrow|H_{soc}|\phi_b\uparrow\rangle = \langle\phi_a\|H_{soc}\|\phi_b\rangle(1/2, 1, 1/2, 0 \mid 1/2, 1/2), \quad (B4)$$

where $\langle\phi_a\|H_{soc}\|\phi_b\rangle$ is the reduced matrix and $(j_1, m_1, j_2, m_2 \mid j, m)$ is the Clebsch-Gordan coefficient. This decomposition, in combination with the equality $(1/2, 1, 1/2, 0 \mid 1/2, 1/2) = -(1/2, 1, -1/2, 0 \mid 1/2, -1/2)$, results in the following relation:

$$\langle\phi_a\uparrow|H_{soc}|\phi_b\uparrow\rangle = -\langle\phi_a\downarrow|H_{soc}|\phi_b\downarrow\rangle. \quad (B5)$$

The above relation can be used to relate among the matrix elements as

$$\begin{aligned} f_{z\uparrow,z\uparrow} &= -f_{z\downarrow,z\downarrow}, \quad f_{z\uparrow,\bar{z}\uparrow} = -f_{z\downarrow,\bar{z}\downarrow}, \quad f_{\bar{z}\uparrow,\bar{z}\uparrow} = -f_{\bar{z}\downarrow,\bar{z}\downarrow}, \\ f_{+\uparrow,+\uparrow} &= -f_{+\downarrow,+\downarrow}, \quad f_{+\uparrow,-\uparrow} = -f_{+\downarrow,-\downarrow}, \\ f_{-\uparrow,-\uparrow} &= -f_{-\downarrow,-\downarrow}. \end{aligned}$$

As a consequence of these relations, the spin-orbit coupling Hamiltonian can be expressed as

$$\begin{aligned} H_{soc} = & f_0(|\phi_+\rangle\langle\phi_+| - |\phi_-\rangle\langle\phi_-|) \otimes \hat{\sigma}_z \\ & + f_1(|\phi_+\rangle\langle\phi_+| - |\phi_-\rangle\langle\phi_-|) \otimes \hat{\sigma}_+ \\ & + f_2(|\phi_z\rangle\langle\phi_z| - |\bar{\phi}_z\rangle\langle\bar{\phi}_z|) \otimes \hat{\sigma}_z \\ & + f_3(|\phi_z\rangle\langle\phi_z| - |\bar{\phi}_z\rangle\langle\bar{\phi}_z|) \otimes \hat{\sigma}_+ + \text{H.c.}, \end{aligned} \quad (B6)$$

with $\hat{\sigma}_z = |\uparrow\rangle\langle\uparrow| - |\downarrow\rangle\langle\downarrow|$, $\hat{\sigma}_+ = |\uparrow\rangle\langle\downarrow|$, and $\hat{\sigma}_- = |\downarrow\rangle\langle\uparrow|$. We impose the invariance under the C_3 operation on H_{soc}, which gives

$$\begin{aligned} C_3 f_0 &= f_0, \quad C_3 f_1 = e^{i2\pi/3}f_1, \quad C_3 f_2 = f_2, \\ C_3 f_3 &= e^{i2\pi/3}f_3. \end{aligned} \quad (B7)$$

Although these matrix elements f_k $(k = 0, \ldots, 3)$ depend on $Q_\pm$, we retain only the zeroth-order, i.e., the nuclear-independent, terms. Then, it is legitimate to discard the noninvariant f_1 and f_3 terms. Furthermore, the f_2 term has the same physical effect as the f_0 term for the coupled translation-rotation systems. Based on this consideration, it is legitimate

to retain the f_0 term, and the relevant spin-orbit coupling Hamiltonian is given by

$$H_{\text{soc}} = \lambda(|\phi_+\rangle\langle\phi_+| - |\phi_-\rangle\langle\phi_-|) \otimes \hat{\sigma}_z, \tag{B8}$$

with the real-valued constant λ.

Here we comment on the $Q_\pm$ dependence of the SOC. If the first-order contribution is incorporated, we have that H_{soc} is given by

$$\begin{aligned} H_{\text{soc}} &= \lambda(|\phi_+\rangle\langle\phi_+| - |\phi_-\rangle\langle\phi_-|) \otimes \hat{\sigma}_z \\ &\quad + (|\phi_+\rangle\langle\phi_+| - |\phi_-\rangle\langle\phi_-|) \otimes (\nu Q_+\hat{\sigma}_+ + \nu^* Q_-\hat{\sigma}_-) \\ &\quad + (|\phi_z\rangle\langle\phi_z| - |\bar{\phi}_z\rangle\langle\bar{\phi}_z|) \otimes (\mu Q_+\hat{\sigma}_+ + \mu^* Q_-\hat{\sigma}_-), \end{aligned} \tag{B9}$$

where ν and μ are the complex numbers. The effects of this term are left for future study.

APPENDIX C: NUMERICAL DETAILS

In this Appendix, we present the details of how to numerically obtain the coupling coefficient $C_{n,m}^{(a,s)}$ of the wave function $|\Psi\rangle = \sum_{a=z,\bar{z},+,-} \sum_{s=\uparrow,\downarrow} \sum_{n,m} C_{n,m}^{(a,s)}|\phi_a, s\rangle|n, m\rangle$ and derive the relation between the coupling coefficients and the observables. To evaluate the matrix elements of the molecular Hamiltonian H, we employ, as the nuclear basis, the eigenstate of the nuclear Hamiltonian H_n [41,42] with the eigenvalue $N\hbar\omega$ with $N = (n - |m|)/2$, which is given for $n = 0, 1, \ldots$ and $m = -n, -n+2, \ldots, n-2, n$, as

$$\begin{aligned} \Gamma_{n,m}(\rho, \varphi) &:= \langle\rho, \varphi|n, m\rangle \\ &= \sqrt{\frac{N!}{\pi(N+|m|)!}} e^{im\varphi} e^{-\rho^2/2} \rho^{|m|} L_N^{|m|}(\rho^2), \end{aligned} \tag{C1}$$

where $L_N^m(x)$ is the associated Laguerre polynomial that satisfies the following differential equation:

$$\left[x\frac{d^2}{dx^2} + (m+1-x)\frac{d}{dx} + N\right]L_N^m(x) = 0. \tag{C2}$$

The matrix element for $\hat{Q}_+$ is computed as

$$\begin{aligned} &\langle n_1, m_1|\hat{Q}_+|n_2, m_2\rangle \\ &= \delta_{m_1, m_2+1}\left(\delta_{n_1, n_2}\sqrt{n_1 + m_1} - \delta_{n_1, n_2-1}\sqrt{n_1 + 1}\right) \end{aligned} \tag{C3}$$

for $m_2 \geqslant 0$ and

$$\begin{aligned} &\langle n_1, m_1|\hat{Q}_+|n_2, m_2\rangle \\ &= \delta_{m_1, m_2+1}\left(\delta_{n_1, n_2}\sqrt{n_1 - m_1 + 1} - \delta_{n_1, n_2+1}\sqrt{n_1}\right) \end{aligned} \tag{C4}$$

for $m_2 < 0$ by using the recurrence relation $L_N^m = L_N^{m+1} - L_{N-1}^{m+1}$ and the integral formula

$$\int_0^\infty dx\, e^{-x} x^m L_M^m(x) L_N^m(x) = \frac{(N+m)!}{N!}\delta_{M,N}. \tag{C5}$$

The matrix element for $\hat{Q}_-$ can be calculated from that for $\hat{Q}_+$ using the relation $\langle n_1, m_2|\hat{Q}_-|n_2, m_2\rangle = \langle n_2, m_2|\hat{Q}_+|n_1, m_1\rangle$.

Expanding H with respect to the electronic basis $\{|\phi_z\rangle, |\bar{\phi}_z\rangle = |\phi_{\bar{z}}\rangle, |\phi_+\rangle, |\phi_-\rangle\}$ and the above nuclear basis

$\{|n, m\rangle\}_{n,m}$ gives the molecular eigenstate

$$|\Psi\rangle = \sum_{a=z,\bar{z},+,-} \sum_{s=\uparrow,\downarrow} \sum_{n,m} C_{n,m}^{(a,s)}|\phi_a, s\rangle|n, m\rangle \tag{C6}$$

or

$$|\Psi(R)\rangle = \langle R|\Psi\rangle = \sum_{a=z,\bar{z},+,-} \sum_{s=\uparrow,\downarrow} C^{(a,s)}(R)|\phi_a, s\rangle \tag{C7}$$

with $C^{(a,s)}(R) \equiv \sum_{n,m} C_{n,m}^{(a,s)}\Gamma_{n,m}(R)$. By using the above expansion, the momentum is expressed as

$$\begin{aligned} \langle\Psi|\hat{p}_z|\Psi\rangle &= \int_0^{2\pi} d\varphi \int_0^\infty d\rho\, \rho\langle\Psi(R)|\hat{p}_z|\Psi(R)\rangle \\ &= \int_0^{2\pi} d\varphi \int_0^\infty d\rho\, \rho\langle\phi_z|\hat{p}_z|\phi_z\rangle \\ &\quad \times \sum_{s=\uparrow,\downarrow}[|C^{(z,s)}(R)|^2 - |C^{(\bar{z},s)}(R)|^2] \\ &= \langle\phi_z|\hat{p}_z|\phi_z\rangle \sum_{s=\uparrow,\downarrow}\sum_{n,m}[|C_{n,m}^{(z,s)}|^2 - |C_{n,m}^{(\bar{z},s)}|^2]. \end{aligned} \tag{C8}$$

In this derivation, the equality $\langle\bar{\phi}_z|\hat{p}_z|\bar{\phi}_z\rangle = -\langle\phi_z|\hat{p}_z|\phi_z\rangle$ and the fact that the rotational basis on the xy plane has no z component, $\hat{p}_z|\phi_\pm\rangle = 0$, are used. Also, the nuclear angular momentum (AM) can be evaluated as

$$\begin{aligned} \langle\Psi|\hat{L}_n|\Psi\rangle &= \int_0^{2\pi} d\varphi \int_0^\infty d\rho\, \rho\langle\Psi(R)|(-i\hbar\partial_\varphi)|\Psi(R)\rangle \\ &= \sum_{a=z,\bar{z},+,-} \sum_{s=\uparrow,\downarrow}\sum_{n,m} m\hbar|C_{n,m}^{(a,s)}|^2. \end{aligned} \tag{C9}$$

APPENDIX D: DETAILS OF LIMITING CASES

In the first limit of $V_0 \to 0$, $\hat{l}_1 := -i\hbar\partial_\varphi - \hbar(|\phi_+\rangle\langle\phi_+| - |\phi_-\rangle\langle\phi_-|)$ is conserved with the integer eigenvalue $l_1/\hbar \in \mathbb{Z}$. The eigenstate with $l_1/\hbar = 0$ is written as

$$\begin{aligned} |\Phi_0\rangle &= a_z(\rho)|\phi_z\rangle + a_{\bar{z}}(\rho)|\bar{\phi}_z\rangle + e^{i\varphi}a_+(\rho)|\phi_+\rangle \\ &\quad + e^{-i\varphi}a_-(\rho)|\phi_-\rangle, \end{aligned} \tag{D1}$$

where the coefficients $a_z, a_{\bar{z}}, a_+, a_-$ are obtained by solving the Schrödinger equation. This state is transformed under the threefold rotation C_3 as

$$\begin{aligned} C_3|\Phi_0\rangle &= a_z|\phi_z\rangle + a_{\bar{z}}|\bar{\phi}_z\rangle + e^{i(\varphi+2\pi/3)}a_+(e^{-i2\pi/3}|\phi_+\rangle) \\ &\quad + e^{-i(\varphi+2\pi/3)}a_-(e^{i2\pi/3}|\phi_-\rangle) \\ &= a_z|\phi_z\rangle + a_{\bar{z}}|\bar{\phi}_z\rangle + e^{i\varphi}a_+|\phi_+\rangle + e^{-i\varphi}a_-|\phi_-\rangle \\ &= |\Phi_0\rangle. \end{aligned} \tag{D2}$$

Thus $|\Phi_0\rangle$ is also the eigenstate of C_3 with the AM quantum number $j = 0$.

The second limit is $V_\pm = 0$, where $\hat{l}_2 := -i\hbar\partial_\varphi + (\hbar/2)(|\phi_+\rangle\langle\phi_+| - |\phi_-\rangle\langle\phi_-|)$ is conserved with the half-odd-integer eigenvalue $l_2/\hbar = \pm(2n-1)/2$ with $n \in \mathbb{N}$. Its eigenstates with $l_2/\hbar = 1/2$ and $-1/2$ are expressed as

$$|\Phi_{1/2}\rangle = b_+(\rho)|\phi_+\rangle + e^{i\varphi}b_-(\rho)|\phi_-\rangle \tag{D3}$$

and

$$|\Phi_{-1/2}\rangle = e^{-i\varphi}c_+(\rho)|\phi_+\rangle + c_-(\rho)|\phi_-\rangle, \tag{D4}$$

respectively. The threefold rotation C_3 transforms these states as

$$C_3|\Phi_{1/2}\rangle = b_+(e^{-i2\pi/3}|\phi_+\rangle) + e^{i(\varphi+2\pi/3)}b_-(e^{i2\pi/3}|\phi_-\rangle)$$

$$= e^{-i2\pi/3}|\Phi_{1/2}\rangle \tag{D5}$$

and

$$C_3|\Phi_{-1/2}\rangle = e^{-i(\varphi+2\pi/3)}c_+(e^{-i2\pi/3}|\phi_+\rangle) + c_-(e^{i2\pi/3}|\phi_-\rangle)$$

$$= e^{i2\pi/3}|\Phi_{-1/2}\rangle. \tag{D6}$$

Thus, as in the first limit, $|\Phi_{\pm 1/2}\rangle$ is also the eigenstate of C_3 with the AM quantum number $j = \pm 1$.

[1] L. D. Barron, *Molecular Light Scattering and Optical Activity*, 2nd ed. (Cambridge University Press, Cambridge, 2004).

[2] S. Mühlbauer, B. Binz, F. Jonietz, C. Pfleiderer, A. Rosch, A. Neubauer, R. Georgii, and P. Böni, Skyrmion lattice in a chiral magnet, Science **323**, 915 (2009).

[3] Y. Togawa, Y. Kousaka, K. Inoue, and J.-i. Kishine, Symmetry, structure, and dynamics of monoaxial chiral magnets, J. Phys. Soc. Jpn. **85**, 112001 (2016).

[4] L. Zhang and Q. Niu, Chiral Phonons at High-Symmetry Points in Monolayer Hexagonal Lattices, Phys. Rev. Lett. **115**, 115502 (2015).

[5] H. Zhu, J. Yi, M.-Y. Li, J. Xiao, L. Zhang, C.-W. Yang, R. A. Kaindl, L.-J. Li, Y. Wang, and X. Zhang, Observation of chiral phonons, Science **359**, 579 (2018).

[6] J. Kishine, A. S. Ovchinnikov, and A. A. Tereshchenko, Chirality-Induced Phonon Dispersion in a Noncentrosymmetric Micropolar Crystal, Phys. Rev. Lett. **125**, 245302 (2020).

[7] M. Kuwata-Gonokami, N. Saito, Y. Ino, M. Kauranen, K. Jefimovs, T. Vallius, J. Turunen, and Y. Svirko, Giant Optical Activity in Quasi-Two-Dimensional Planar Nanostructures, Phys. Rev. Lett. **95**, 227401 (2005).

[8] G. L. J. A. Rikken, C. Strohm, and P. Wyder, Observation of Magnetoelectric Directional Anisotropy, Phys. Rev. Lett. **89**, 133005 (2002).

[9] Y. Tokura and N. Nagaosa, Nonreciprocal responses from noncentrosymmetric quantum materials, Nat. Commun. **9**, 3740 (2018).

[10] B. Göhler, V. Hamelbeck, T. Z. Markus, M. Kettner, G. F. Hanne, Z. Vager, R. Naaman, and H. Zacharias, Spin selectivity in electron transmission through self-assembled monolayers of double-stranded DNA, Science **331**, 894 (2011).

[11] D. Mishra, T. Z. Markus, R. Naaman, M. Kettner, B. Göhler, H. Zacharias, N. Friedman, M. Sheves, and C. Fontanesi, Spin-dependent electron transmission through bacteriorhodopsin embedded in purple membrane, Proc. Natl. Acad. Sci. USA **110**, 14872 (2013).

[12] M. Kettner, B. Göhler, H. Zacharias, D. Mishra, V. Kiran, R. Naaman, C. Fontanesi, D. H. Waldeck, S. Sęk, J. Pawłowski, and J. Juhaniewicz, Spin filtering in electron transport through chiral oligopeptides, J. Phys. Chem. C **119**, 14542 (2015).

[13] Z. Xie, T. Z. Markus, S. R. Cohen, Z. Vager, R. Gutierrez, and R. Naaman, Spin specific electron conduction through DNA oligomers, Nano Lett. **11**, 4652 (2011).

[14] M. Kettner, V. V. Maslyuk, D. Nürenberg, J. Seibel, R. Gutierrez, G. Cuniberti, K.-H. Ernst, and H. Zacharias, Chirality-dependent electron spin filtering by molecular monolayers of helicenes, J. Phys. Chem. Lett. **9**, 2025 (2018).

[15] M. Suda, Y. Thathong, V. Promarak, H. Kojima, M. Nakamura, T. Shiraogawa, M. Ehara, and H. M. Yamamoto, Light-driven molecular switch for reconfigurable spin filters, Nat. Commun. **10**, 2455 (2019).

[16] K. Banerjee-Ghosh, O. Ben Dor, F. Tassinari, E. Capua, S. Yochelis, A. Capua, S.-H. Yang, S. S. P. Parkin, S. Sarkar, L. Kronik, L. T. Baczewski, R. Naaman, and Y. Paltiel, Separation of enantiomers by their enantiospecific interaction with achiral magnetic substrates, Science **360**, 1331 (2018).

[17] T. S. Metzger, S. Mishra, B. P. Bloom, N. Goren, A. Neubauer, G. Shmul, J. Wei, S. Yochelis, F. Tassinari, C. Fontanesi, D. H. Waldeck, Y. Paltiel, and R. Naaman, The electron spin as a chiral reagent, Angew. Chem., Int. Ed. **59**, 1653 (2020).

[18] A. Inui, R. Aoki, Y. Nishiue, K. Shiota, Y. Kousaka, H. Shishido, D. Hirobe, M. Suda, J.-i. Ohe, J.-i. Kishine, H. M. Yamamoto, and Y. Togawa, Chirality-Induced Spin-Polarized State of a Chiral Crystal CrNb$_3$S$_6$, Phys. Rev. Lett. **124**, 166602 (2020).

[19] Y. Nabei, D. Hirobe, Y. Shimamoto, K. Shiota, A. Inui, Y. Kousaka, Y. Togawa, and H. M. Yamamoto, Current-induced bulk magnetization of a chiral crystal CrNb$_3$S$_6$, Appl. Phys. Lett. **117**, 052408 (2020).

[20] K. Shiota, A. Inui, Y. Hosaka, R. Amano, Y. Ōnuki, M. Hedo, T. Nakama, D. Hirobe, J.-i. Ohe, J.-i. Kishine, H. M. Yamamoto, H. Shishido, and Y. Togawa, Chirality-Induced Spin Polarization over Macroscopic Distances in Chiral Disilicide Crystals, Phys. Rev. Lett. **127**, 126602 (2021).

[21] R. Naaman and D. H. Waldeck, Chiral-induced spin selectivity effect, J. Phys. Chem. Lett. **3**, 2178 (2012).

[22] R. Naaman, Y. Paltiel, and D. H. Waldeck, Chiral molecules and the electron spin, Nat. Rev. Chem. **3**, 250 (2019).

[23] R. Naaman, Y. Paltiel, and D. H. Waldeck, Chiral molecules and the spin selectivity effect, J. Phys. Chem. Lett. **11**, 3660 (2020).

[24] F. Evers, A. Aharony, N. Bar-Gill, O. Entin-Wohlman, P. Hedegård, O. Hod, P. Jelinek, G. Kamieniarz, M. Lemeshko, K. Michaeli, V. Mujica, R. Naaman, Y. Paltiel, S. Refaely-Abramson, O. Tal, J. Thijssen, M. Thoss, J. M. van Ruitenbeek, L. Venkataraman, D. H. Waldeck, B. Yan, and L. Kronik, Theory of chirality induced spin selectivity progress and challenges, Adv. Mater. **34**, 2106629 (2022).

[25] A.-M. Guo and Q.-f. Sun, Spin-Selective Transport of Electrons in DNA Double Helix, Phys. Rev. Lett. **108**, 218102 (2012).

[26] A.-M. Guo and Q.-F. Sun, Spin-dependent electron transport in protein-like single-helical molecules, Proc. Natl. Acad. Sci. USA **111**, 11658 (2014).

[27] S. Matityahu, Y. Utsumi, A. Aharony, O. Entin-Wohlman, and C. A. Balseiro, Spin-dependent transport through a chiral molecule in the presence of spin-orbit interaction and nonunitary effects, Phys. Rev. B **93**, 075407 (2016).

[28] J. H. Bardarson, A proof of the Kramers degeneracy of transmission eigenvalues from antisymmetry of the scat-

tering matrix, J. Phys. A: Math. Theor. **41**, 405203 (2008).

[29] Y. Utsumi, O. Entin-Wohlman, and A. Aharony, Spin selectivity through time-reversal symmetric helical junctions, Phys. Rev. B **102**, 035445 (2020).

[30] J. Fransson, Chirality-induced spin selectivity: The role of electron correlations, J. Phys. Chem. Lett. **10**, 7126 (2019).

[31] G.-F. Du, H.-H. Fu, and R. Wu, Vibration-enhanced spin-selective transport of electrons in the DNA double helix, Phys. Rev. B **102**, 035431 (2020).

[32] L. Zhang, Y. Hao, W. Qin, S. Xie, and F. Qu, Chiral-induced spin selectivity: A polaron transport model, Phys. Rev. B **102**, 214303 (2020).

[33] J. Fransson, Vibrational origin of exchange splitting and chiral-induced spin selectivity, Phys. Rev. B **102**, 235416 (2020).

[34] S. Alwan and Y. Dubi, Spinterface origin for the chirality-induced spin-selectivity effect, J. Am. Chem. Soc. **143**, 14235 (2021).

[35] I. Bersuker, *The Jahn-Teller Effect* (Cambridge University Press, Cambridge, 2006).

[36] I. B. Bersuker, Jahn-Teller and pseudo-Jahn-Teller effects: From particular features to general tools in exploring molecular and solid state properties, Chem. Rev. (Washington, DC) **121**, 1463 (2021).

[37] S. V. Streltsov and D. I. Khomskii, Jahn-Teller Effect and Spin-Orbit Coupling: Friends or Foes?, Phys. Rev. X **10**, 031043 (2020).

[38] K. Wang and T. Zeng, Hamiltonian formalism of spin-orbit Jahn-Teller and pseudo-Jahn-Teller problems in trigonal and tetragonal symmetries, Phys. Chem. Chem. Phys. **21**, 18939 (2019).

[39] T. Zeng, R. J. Hickman, A. Kadri, and I. Seidu, General formalism of vibronic Hamiltonians for tetrahedral and octahedral systems: Problems that involve T, E states and t, e vibrations, J. Chem. Theory Comput. **13**, 5004 (2017).

[40] S. Mishra, A. K. Mondal, S. Pal, T. K. Das, E. Z. B. Smolinsky, G. Siligardi, and R. Naaman, Length-dependent electron spin polarization in oligopeptides and DNA, J. Phys. Chem. C **124**, 10776 (2020).

[41] H. Koizumi and S. Sugano, The geometric phase in two electronic level systems, J. Chem. Phys. **101**, 4903 (1994).

[42] R. Requist, F. Tandetzky, and E. K. U. Gross, Molecular geometric phase from the exact electron-nuclear factorization, Phys. Rev. A **93**, 042108 (2016).

[43] P. B. Allen, A. G. Abanov, and R. Requist, Quantum electrical dipole in triangular systems: A model for spontaneous polarity in metal clusters, Phys. Rev. A **71**, 043203 (2005).

[44] Y. Wu and J. E. Subotnik, Electronic spin separation induced by nuclear motion near conical intersections, Nat. Commun. **12**, 700 (2021).

[45] X. Bian, Y. Wu, H.-H. Teh, Z. Zhou, H.-T. Chen, and J. E. Subotnik, Modeling nonadiabatic dynamics with degenerate electronic states, intersystem crossing, and spin separation: A key goal for chemical physics, J. Chem. Phys. **154**, 110901 (2021).

[46] T. Furukawa, Y. Shimokawa, K. Kobayashi, and T. Itou, Observation of current-induced bulk magnetization in elemental tellurium, Nat. Commun. **8**, 954 (2017).

[47] T. Yoda, T. Yokoyama, and S. Murakami, Orbital Edelstein effect as a condensed-matter analog of solenoids, Nano Lett. **18**, 916 (2018).